Ultra-Low loss and compact coplanar waveguide crossing

Amir Hosseini[a], Yang Zhang[b], and Ray T. Chen[b]

[a] Omega Optics, Inc., 10306 Sausalito Dr, Austin, TX 78759, USA

[b] Department of Electrical and Computer Engineering, the University of Texas at Austin, Austin, TX, 78758, USA

ABSTRACT

We investigate the loss mechanism in 3-moded multimode-interference couplers that are the building blocks of a compact and low-loss waveguide crossing structure. Broadband silicon waveguide crossing arrays with <0.01dB insertion loss per crossing are proposed using cascaded multimode interference couplers, where lateral subwavelength nanostructures are used to reduce the insertions loss. We design and fabricate a 101×101 waveguide crossing array with a pitch of 3.08μm. Insertion loss of ~0.02dB per crossing and crosstalk <-40dB at 1550nm operating wavelength and broad transmission spectrum ranging from 1520 to 1610nm are experimentally demonstrated.

Keywords: Silicon photonics, waveguide theory, multimode interference coupler

1. INTRODUCTION

Efficient waveguide crossings are required to materialize full potential of silicon photonics for on-chip optical interconnects. Single mode silicon waveguide crossings with normal intersections result in over 1dB loss and ~-10dB cross-talk due to the high index contrast of the silicon-on-insulator (SOI) platform [1, 2]. This issue has been addressed by several groups over the past decade. Subwavelength gratings in silicon waveguides have been used to lower the effective refractive index at the crossing resulting in insertion loss as low as 0.023dB and <-40dB cross-talk [1]. However, this structure requires ~10μm long adiabatic tapers to gradually reduce the effective refractive index with near 0.3dB loss per taper. Also, the reduced effective refractive index (<2) is accompanied by the mode profile extending several microns laterally, which in turn increases the waveguide pitch in a cross-grid structure. As another approach, low-Q resonator based crossings suffer from limited optical bandwidth (10-15nm) [3]. Vertically integrated silicon nitride waveguides over SOI waveguides have been shown to reduce the cross-talk to <-44dB [4], however, the required fabrication process is more complicated than that of single layer Photonic Integrated Circuits (PICs).

On the other hand, multimode interference (MMI) based crossings with relatively compact sizes (13x13μm2) have been demonstrated with insertion loss of ~0.2dB [2] [5]. In this type of structures, the self-focusing effect of the MMI is used to form a single image of the MMI input waveguide mode profile at the crossing thus minimizing the effect of the crossing waveguide on the mode profile. Recently, using 2D finite difference time domain (FDTD) simulations it was theoretically shown that a periodic structure formed by cascading multimode focusing sections can support a low-loss Bloch wave [6]. In addition to the fact that this structure can potentially lower the insertion loss to 0.04dB per crossing, a waveguide pitch of ~3μm also enables compact waveguide crossing arrays. In this paper we show that a compact periodic structure formed by cascading MMIs with engineered lateral cladding refractive index can lead to less than 0.01dB loss per crossing allowing integration of 100s of waveguide crossings with minimal insertion loss and cross-talk.

Optical Interconnects XIV, edited by Henning Schröder, Ray T. Chen, Alexei L. Glebov,
Proc. of SPIE Vol. 8991, 89910X · © 2014 SPIE · CCC code: 0277-786X/14/$18
doi: 10.1117/12.2044227

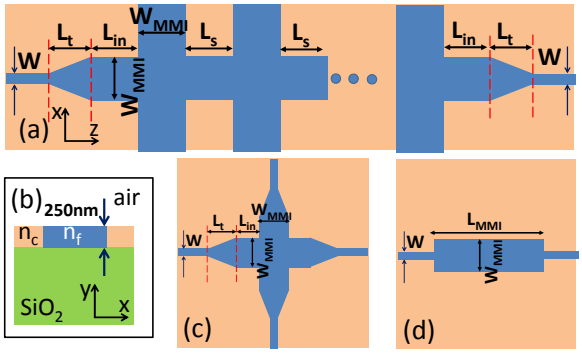

Figure 1. (a) A top view schematic of the cascaded multimode interference based waveguide crossings, (b) a side view schematic of the waveguide structure with lateral cladding indicated, (c) a single waveguide crossing structure, (d) a 1×1 MMI.

2. DESIGN AND DISCUSSION

The platform is a SOI substrate with 3μm thick buried oxide (BOX) layer and 250nm thick top silicon layer (n_f=3.47). A schematic of the waveguide array crossing structure is shown in Figure 1(a-b). This arrayed structure may be thought as a cascaded MMI based waveguide crossing shown in Figure 1(c), in which, according to the self-imaging principle of multimode waveguides, images of the input field are periodically formed along the multimode waveguide. It has been proposed that the multimode waveguide can be crossed by another one at the points where single-fold images are formed [2].

In order to design a low-loss waveguide crossing array, we first investigate the loss mechanism in a simple 1×1 symmetric MMI structure shown in Figure 1(d). Similar to a previously reported design [6], here we assume the multimode waveguide width, W_{MMI}=1.2μm, and input/output single mode waveguide width, W=0.6μm. Note that the MMI region only supports three TE polarized modes. So far, the MMI insertion loss has been explained by the modal phase errors in the multimode waveguide [7-9].

For an ideal self-imaging it is required that $\beta_{m,ideal} = \beta_0 - m(m+2)\pi/3L_\pi$, where $\beta_m$is the propagation constant of mode m, and L_π is the beat length of self-imaging process [10]. Following the analysis in [7] one can write

$$\beta_m = \beta_0\sqrt{1+\frac{K_{T0}^2-K_{Tm}^2}{\beta_0}} \qquad (1)$$

where, $K_{Tm} = (m+1)\pi/W_{em}$ is the transverse wave number of mode m, and W_{em} is the effective width of the MMI for the m^{th} mode. The modal phase error is given as $\Delta\varphi_m = L_{MMI}\Delta\beta_m = L_{MMI}(\beta_m - \beta_{m,ideal})$, where L_{MMI} is the MMI length. It has been shown that the lateral cladding index (n_c) [see Fig. 1(b)] can be tuned to minimize $\Delta\varphi_m$ for a few number of dominant modes. Particularly, at the N-folding imaging length $\Delta\varphi_m$ is given as

$$\Delta\varphi_m \approx (P/4)\frac{\lambda_0^2(m+1)^4\pi}{2Nn_f^2W_{e0}^2}\left[\frac{1}{8}-\frac{\lambda_0 n_{f2D}^2}{6\pi W_{e0}(n_{f2D}^2-n_{c2D}^2)^2}\right] \qquad (2)$$

where, λ_0 is the optical wavelength and P is the number of self-imaging periods. We added the multiplier P/4 to the modal phase error presented in [8], since we have a symmetric interference here (required MMI length is divided by 4 [9]), and P=2 in the MMI crossing structure. Also, we note that n_{f2D}=2.9 and n_{c2D} are the effective refractive indices of the fundamental mode of an infinite slab waveguide with the same thickness as the MMI (250nm) and core refractive and cladding indices of n_f and n_c, respectively.

While tuning the lateral cladding index (n_c) is generally applicable to MMIs that support several modes in their multimode region, we notice that the multimode waveguide shown in Fig. 1(d) only supports 3 modes (0^{th}, 1^{st} and 2^{nd}), among which the odd 1^{st} order mode is not excited to due to the symmetry of the structure. That leaves only 2 modes (m=0 and m=2), for which the self-imaging condition is simply reduced to

$\beta_0 - \beta_2 = 2\pi n/L_{MMI}$, n: integer (3)

One notes that for any W_{MMI} and n_c, as long as only the 0th and the 2nd modes are excited, there is always an MMI length for which this condition can be perfectly satisfied. In other words, the remaining phase error ($\Delta\varphi_2$) can be in theory completely eliminated by tuning L_{MMI}.

In order to confirm this observation, we simulate different 1×1 MMI structures shown in Figure 2 (a-c) using 3D PhotonDesign FIMMPROP, an eigenmode decomposition based simulator. Linear tapers (L_t=1μm) are used in Figure 2 (b-c) for high transmissions as suggested by Chen et al [5]. In each case, we sweep the MMI lengths, L_{MMI}, L, L_{in} for MMIs shown in Figure 2 (a-c), respectively, and find the maximum transmission. Figure 2 (c) shows optical transmission as a function of n_c. As n_c increases, the transmission improves in all cases. Interestingly, the 1×1 MMI with tapers and without crossing is essentially loss-less and the 1×1 MMI without tapers has the worst performance. Since the modal phase errors are not applicable in any of these cases, we need to consider a different loss mechanism.

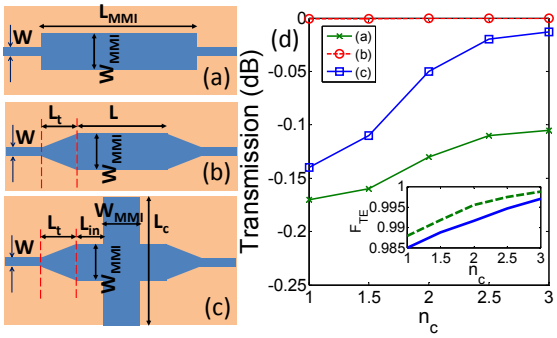

Figure 2. Schematics of simulated structures, (a) 1×1 MMI with single mode access waveguides, (b) 1×1 MMI with tapered input output transitions, (c) MMI waveguide crossing using 1×1 MMI with tapered input output transition, (d) simulated transmission versus lateral cladding index (nc) for the structure in (a-c), (d) inset shows TE fraction versus nc for the fundamental mode in the single mode access waveguide (width=0.6μm, solid blue curve) and the second order mode in the MMI region (width=1.2μm, dashed green line).

In the structure shown in Fig. 2 (a), we note that the fundamental mode in the single mode access waveguide, and the 2nd order mode in the multimode region are both quasi TE modes with considerable amount of TM polarization (~1.5%) for n_c=1 as shown in inset of Fig. 2 (d). Here, the TE (TM) fraction is the fraction of the Poynting vector with horizontal (vertical) electric field

$$F_{TE} = \frac{\int E_x H_y ds}{\int P_z ds} \quad (4)$$

As n_c increases, both of these modes become essentially completely TE (FTE~100%) and power transmission between the two waveguides improves at the input and output. The tapers help improving the power transmission by avoiding sharp transitions and by reducing the portion of the power in the 2nd order mode in the multimode region [5]. Similarly, when we compare the tapered MMIs with and without waveguide crossings, we note that the crossing section is much wider compared to the MMI width (L_c>>WMMI), this section can be thought of as a slab waveguide that supports pure TE modes. When n_c increases from 1 to 2.5, the two excited modes in the MMI region also become nearly pure TE and the power transmission between the two section increases. Thus, we conclude that the main loss in the 3-moded MMI structures is due to coupling loss at sharp transitions and not due to modal phase errors.

3. TEST RESULTS

We fabricate waveguide arrays normally crossed by other waveguide arrays as shown in Fig. 3(a) using both conventional MMI crossings and index-engineered MMI crossings. In order to implement n_c>1, subwavelength nanostructure (SWN) is used to engineer the lateral cladding refractive index [8]. The SWN is periodic along the light propagation direction, and its refractive index (nSWN) can be engineered by tuning the filling factor (ff) of air trench inside the SWN, which is defined as the ratio between the air trench width (W) and the SWN period (Λ). We use Λ=200nm for the SWN to fabricate devices with W=30, 40, 50, 60, 70 and 80nm. The width of the SWN is 200nm to accommodate the field penetration into the lateral cladding.

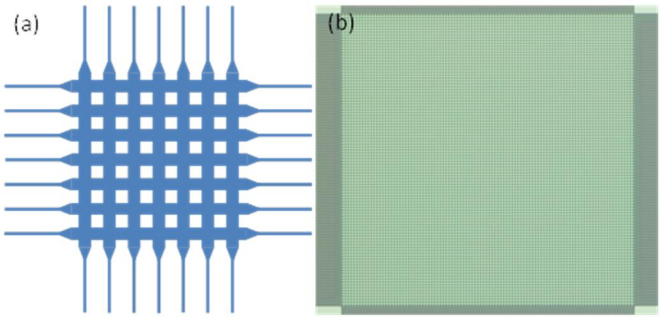

Fig. 3. (a) Schematic of a cross-grid MMI based waveguide array crossing. 7×7 cross-grid is shown for simplicity. (b) an optical microscope image of the fabricated 101×101 cross-grid.

The designed structures are fabricated on a SOI wafer using electron beam lithography (EBL) and reactive ion etching (RIE). MMI crossings with and without SWN are used in the cross-grids for comparison. Fig. 3(b) shows an optical microscope image of the fabricated 101×101 cross-grid with index-engineered MMI crossings. Figs. 4(a-b) and (c-d) show scanning electron microscope (SEM) images of the MMI crossings, with and without SWN, respectively.

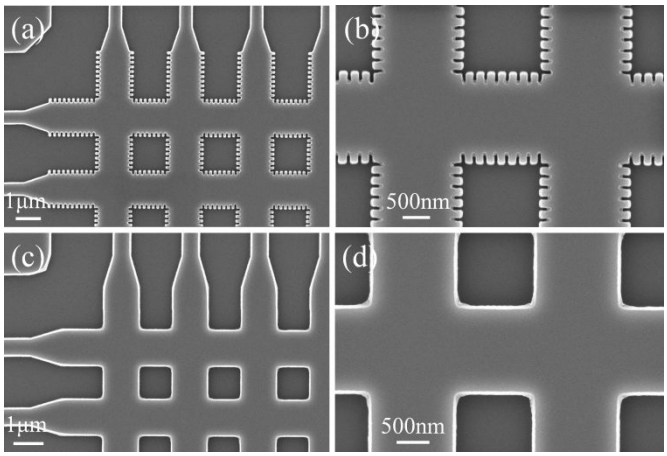

Fig. 4. SEM images of the fabricated waveguide array crossings with (a-b) and without (c-d) index engineering of the lateral claddings.

Transverse electric (TE) polarized light from a broadband amplified spontaneous emission (ASE) light source is coupled in and out of the cross-grid using SWN based grating couplers [10]. The transmissions obtained from the cross-grid are normalized to the transmission of a reference waveguide with the same propagation length. We experimentally find that the index-engineered MMI crossing with W=50nm had the best performance. Fig. 5 shows the normalized transmissions of the 101x101 cross-grids for a horizontal waveguide in the middle of the grid (the 51th waveguide) with both the index-engineered (n_c=2.5, with SWN) and conventional (n_c=1, no SWN) MMI crossings. The cross-talk measured from a vertical waveguide in the middle of the grid (the 51th waveguide) for index-engineered structure is also shown in Fig. 5.

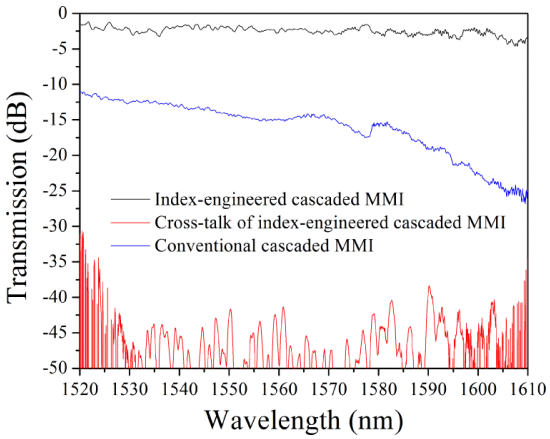

Fig. 5. Measured transmission for 101 cascaded MMI crossings with (black) and without (blue) index-engineering, and the cross-talk of index-engineered MMI crossing.

The results show that the conventional MMI crossing has an insertion loss of 0.14dB at 1550nm operating wavelength, which is comparable to what demonstrated in ref. [2]. The index-engineered MMI crossing has an insertion loss of 0.019dB at 1550nm operating wavelength. The cross-talk signal is below the noise floor of our testing system, so the exact cross-talk cannot be extracted from the transmission. However, the estimated cross-talk is at least below -40dB over 1530-1600nm wavelength range. Besides the ultra-low insertion loss and low cross-talk, cascading index-engineered MMI crossings enable a waveguide pitch of 3.08μm in a cross-grid, which is the most compact footprint for a non-resonant crossing to our knowledge.

4. CONCLUSIONS

In conclusion, while the high-index-contrast of the SOI platform allows small footprints for photonic devices, it also makes excess loss reduction and cross-talk suppression challenging. An ultra-low loss waveguide crossing structure with a waveguide pitch of only 3.08μm has been demonstrated on the SOI platform. The crossing structure, utilizing cascaded index-engineered MMIs, has an insertion loss of 0.019dB and crosstalk lower than -40dB at 1550 operating wavelength, and broad transmission spectrum of over more than 90nm bandwidth.

5. REFERENCE

1. P. J. Bock, P. Cheben, J. H. Schmid, J. Lapointe, A. Delâge, D.-X. Xu, S. Janz, A. Densmore, and T. J. Hall, Optics express 18, 16146-16155 (2010).
2. H. Chen and A. W. Poon, Photonics Technology Letters, IEEE 18, 2260-2262 (2006).
3. C. Manolatou and H. A. Haus, in Passive Components for Dense Optical Integration (Springer, 2002), pp. 97-125.
4. A. M. Jones, C. T. DeRose, A. L. Lentine, D. C. Trotter, A. L. Starbuck, and R. A. Norwood, Optics express 21, 12002-12013 (2013).
5. C.-H. Chen and C.-H. Chiu, Quantum Electronics, IEEE Journal of 46, 1656-1661 (2010).
6. M. Popovic, E. P. Ippen, and F. Kartner, in Lasers and Electro-Optics Society, 2007. LEOS 2007. The 20th Annual Meeting of the IEEE, (IEEE, 2007), 56-57.
7. J. Huang, R. Scarmozzino, and R. Osgood Jr, Photonics Technology Letters, IEEE 10, 1292-1294 (1998).
8. A. Ortega-Monux, L. Zavargo-Peche, A. Maese-Novo, I. Molina-Fernández, R. Halir, J. Wanguemert-Perez, P. Cheben, and J. Schmid, Photonics Technology Letters, IEEE 23, 1406-1408 (2011).
9. A. Hosseini, D. N. Kwong, Y. Zhang, H. Subbaraman, X. Xu, and R. T. Chen, Selected Topics in Quantum Electronics, IEEE Journal of 17, 510-515 (2011).
10. X. Xu, H. Subbaraman, J. Covey, D. Kwong, A. Hosseini, and R. T. Chen, Applied physics letters 101, 031109-031109-031104 (2012).